

Fig. 1. Jimthompsonite. **(a)** Triple A-chain projected onto (100). The inner parts of the chain are very straight, while the outer parts are slightly O-rotated. **(b)** Structure projected onto (001). The stacking sequence is $++--$. B-chains occur between octahedral layers of like skew, while

A-chains are between layers of opposite skew. The basal oxygen layers of the silicate chains are warped out of the (100) plane. The c -glide and b -glide are labeled g_c and g_b . M5 is indicated by solid circles and the unit cell is outlined [78V2].

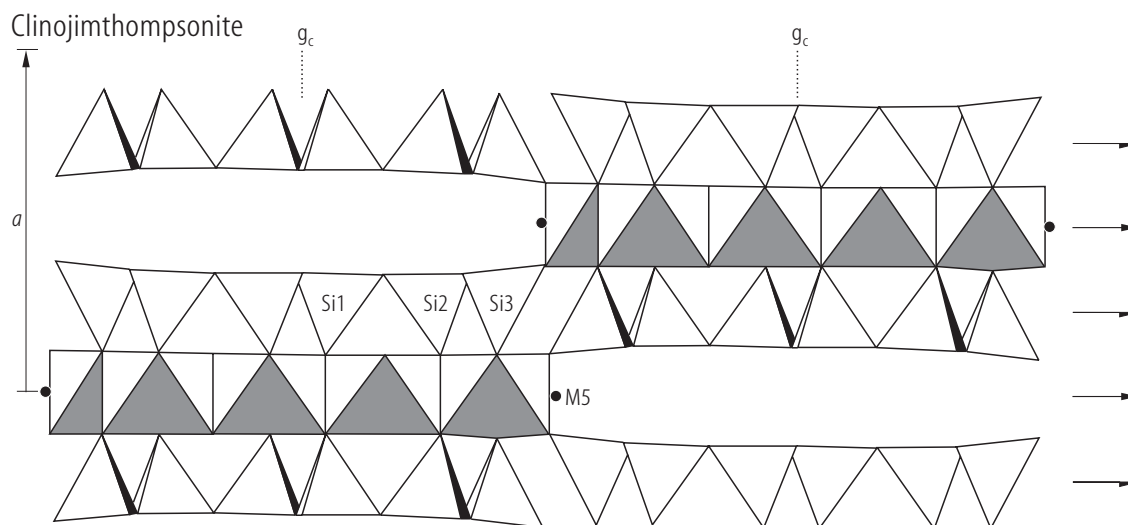


Fig. 2. Clinojimthompsonite. c -axis projection of the structure. The stacking sequence is + + + + and all triple chains are symmetrically equivalent. As in jimthompsonite, the basal oxygen layers of the silicate chains are warped out of the (100) plane [78V2].

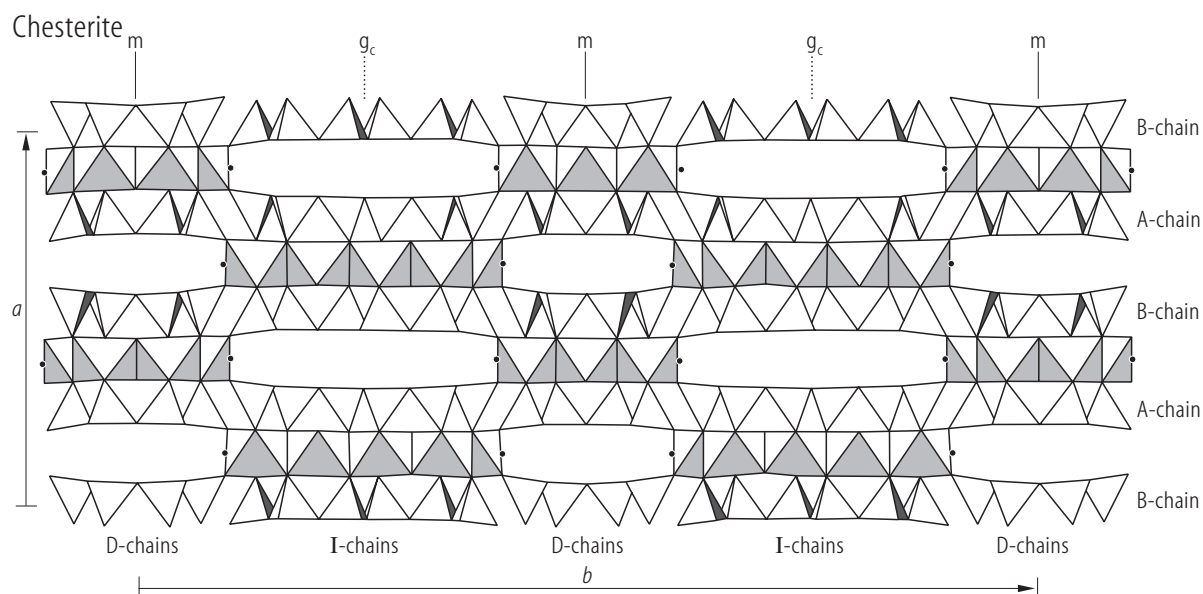


Fig. 3. Chesterite. (001) projection of the structure. The stacking sequence is + + - - and I-beams with double and triple B-chains are sandwiched between octahedral layers of like skew, while double and triple A-chains are between layers

of opposite skew. Basal oxygen layers of all silicate chains are warped out of the (100) plane [78V2]. Atoms in the triple chain I-beams are denoted by T and those in the double -chain I-beams by D.

Babingtonite

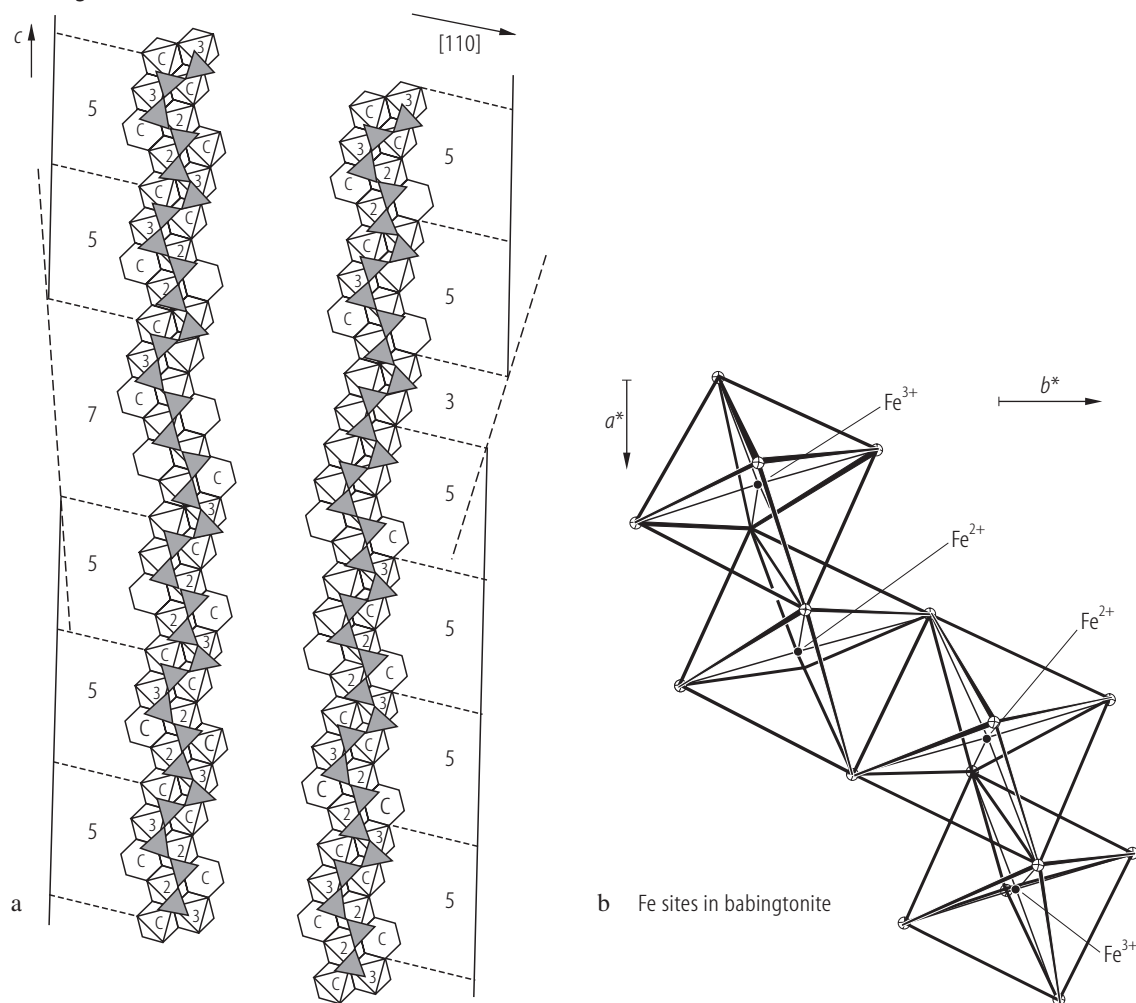


Fig. 4. Babingtonite. **(a)** Schematic representation of the structure [81C1, 91B1]. The projection along [110] shows the repeat sequence of five tetrahedra in the silicate chain occurring in the ideal structure. Note the ideal sequence of cations in the staggered bands of eight edge-shared coordination polyhedra, $\text{Ca-Fe}^{3+}\text{-Ca-Fe}^{2+}\text{-Fe}^{2+}\text{-Ca-Fe}^{3+}\text{-Ca}$ and zig-zag tetramers of edge-shared FeO_6 octahedra

(labeled as 3-2-2-3) which are separated by the Ca polyhedra (C). These sequences become disrupted by chain periodicity faults. For example, "siebener" linkages shorten (left) and "dreier" linkages elongate (right) the sequences of edge-shared FeO_6 octahedra. **(b)** Projection of the Fe-O octahedra onto the $(a^* b^*)$ plane [80A1].

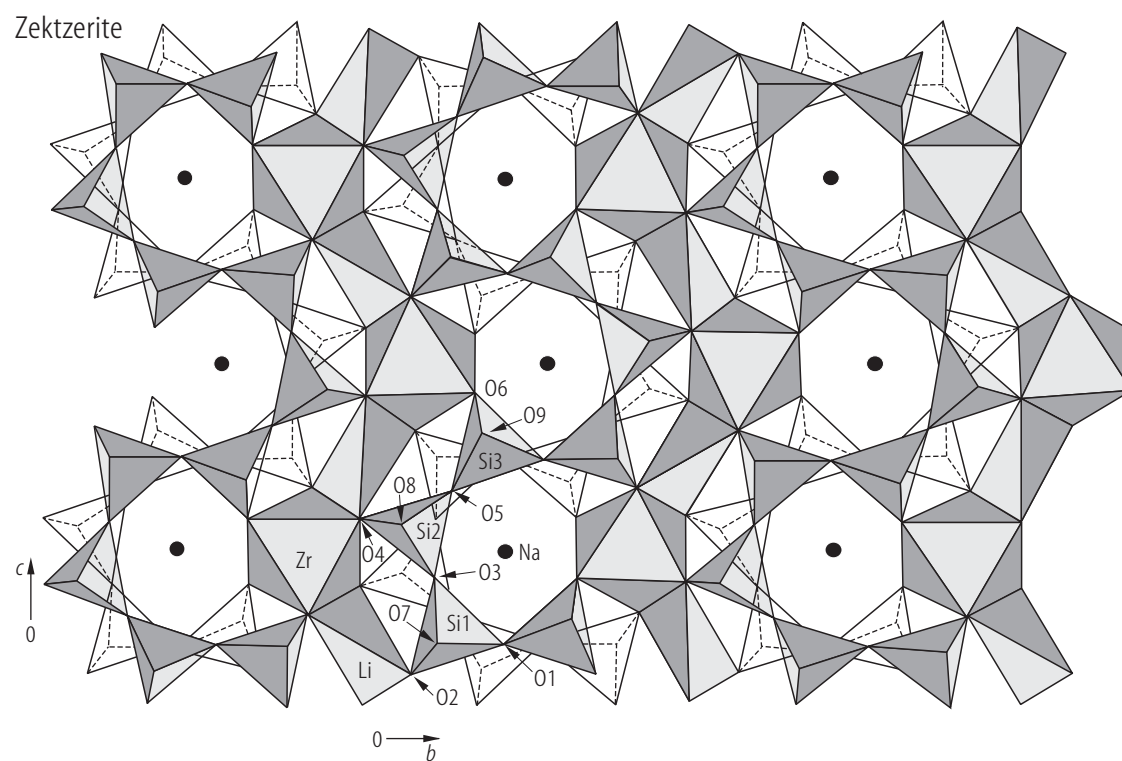


Fig. 5. Zektzerite. A view of one-half of the structure projected along $[100]$; the second half is obtained by reflection across a mirror plane (at $x = 1/2$) passing through the oxygen atoms O7, O8 and O9, thereby doubling the silicate chain [78G1].

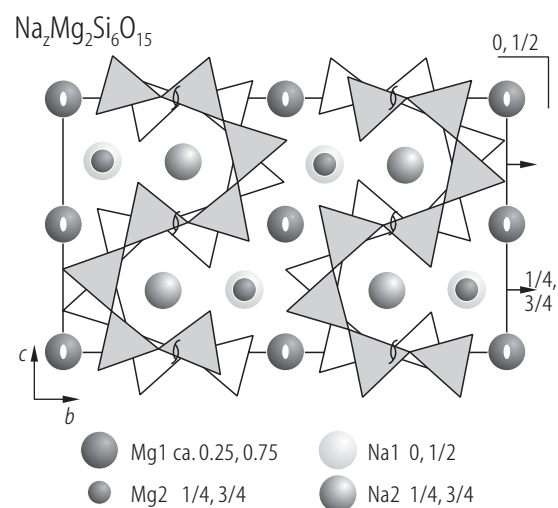


Fig. 6. $\text{Na}_2\text{Mg}_2\text{Si}_6\text{O}_{15}$. Crystal structure projected along a [72C1].

Batisite

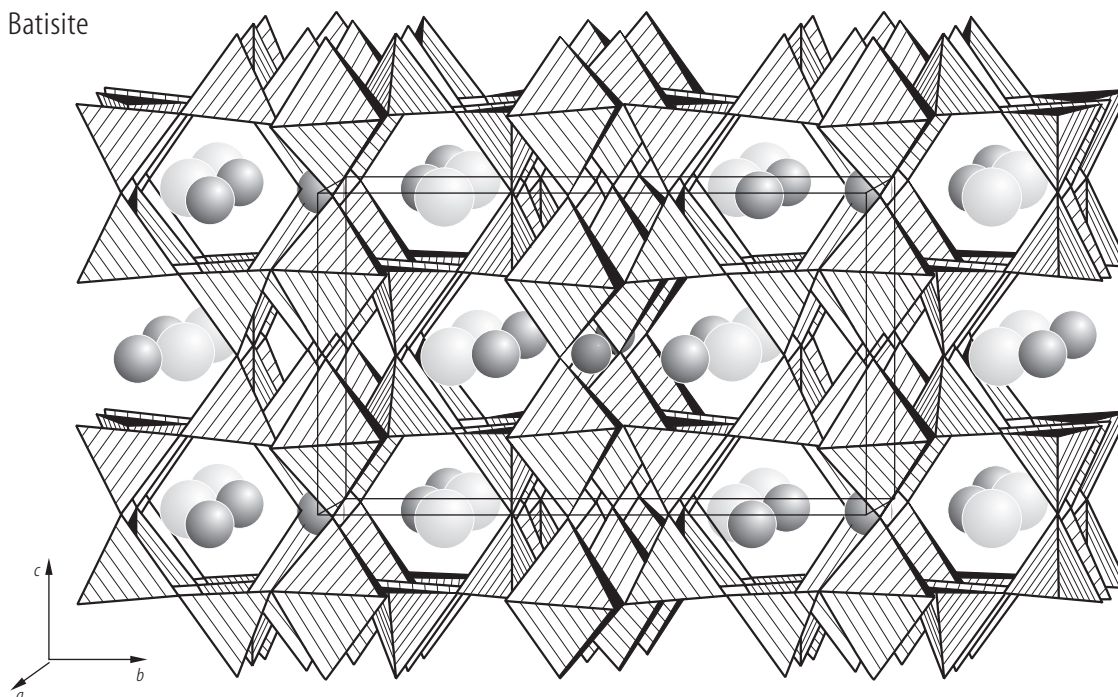
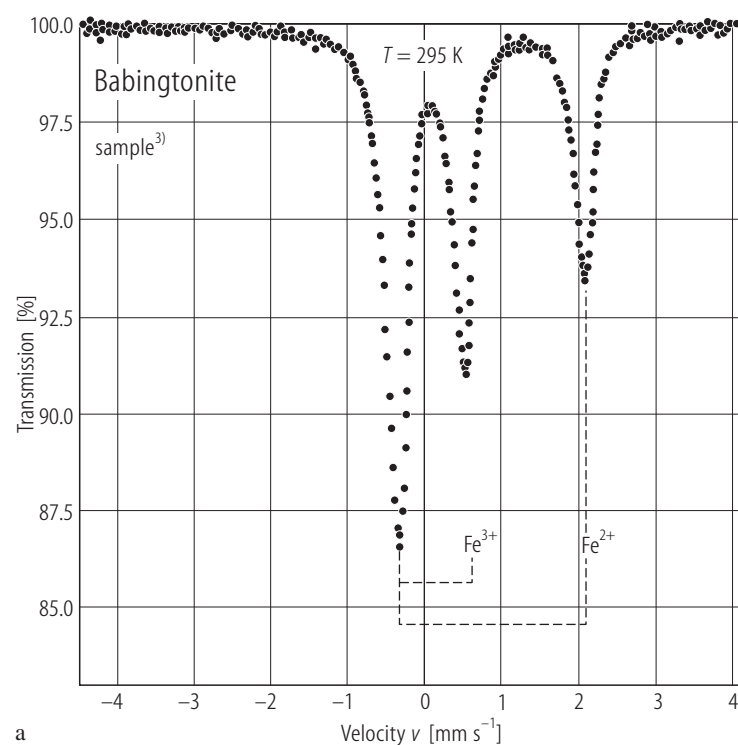
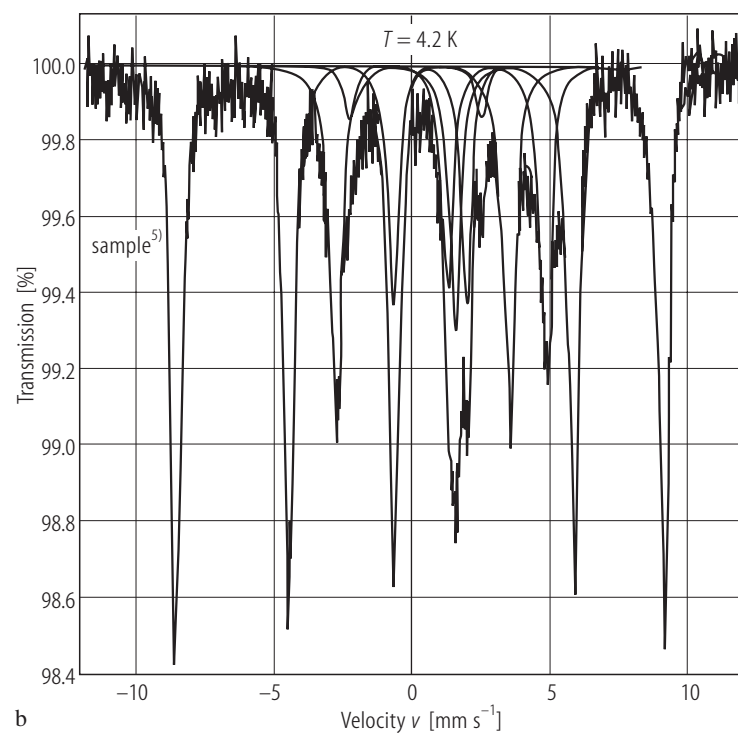


Fig. 7. Batisite. View approximately along [100]. Framework of $(\text{Ti,Fe,Nb,Zr})\text{O}_6$ octahedra and SiO_4 -tetrahedra sharing corners (hatched polyhedral representation). Channels and voids occupied by large cations. Small circles: Na positions; intermediate circles: Cat2; biggest circles: Cat1[87S1].



a



b

Fig. 8. Babingtonite. ^{57}Fe NGR spectra at room temperature **(a)** for sample ³⁾ [80A1] and at 4.2 K **(b)** for sample ⁵⁾ [91B1]. For compositions of samples ³⁾ and ⁵⁾ see Table 5.

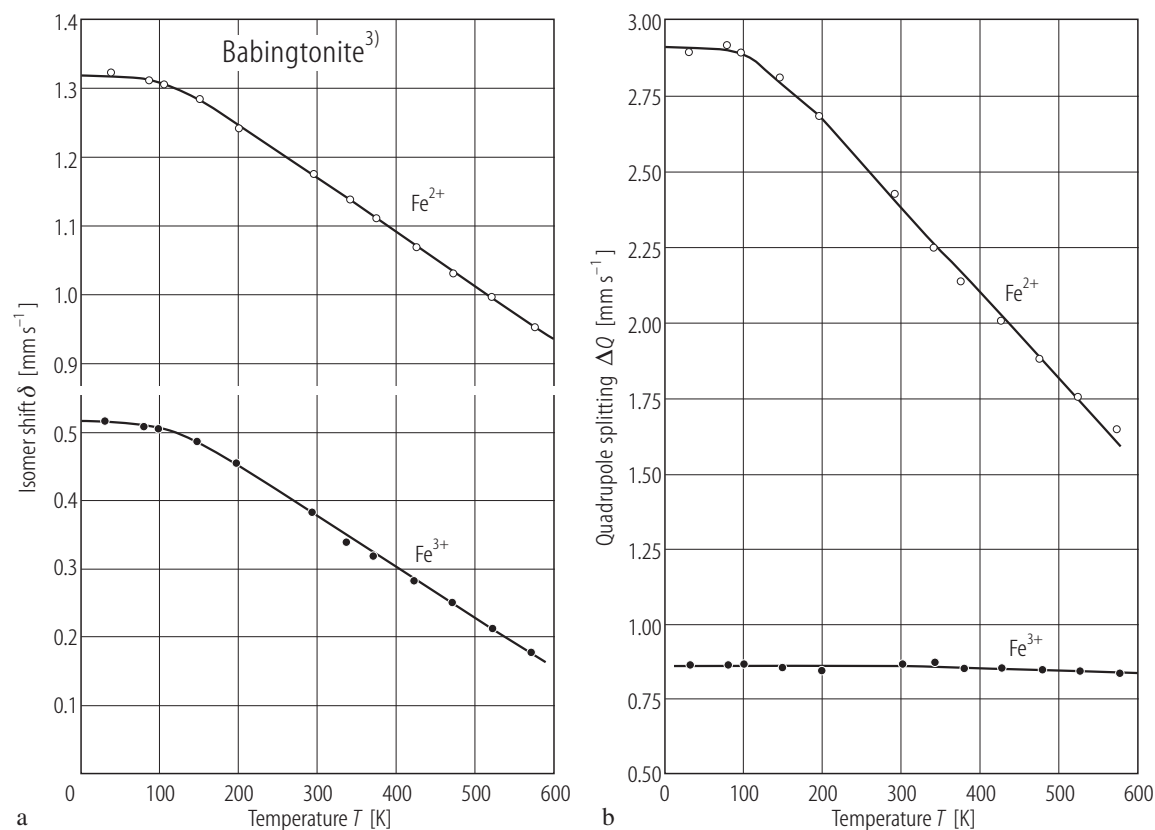


Fig. 9. Babingtonite³⁾. Temperature dependences of the isomer shifts (relative to α -Fe) (a) and of the quadrupole splitting (b) for Fe²⁺ and Fe³⁺ [80A1].

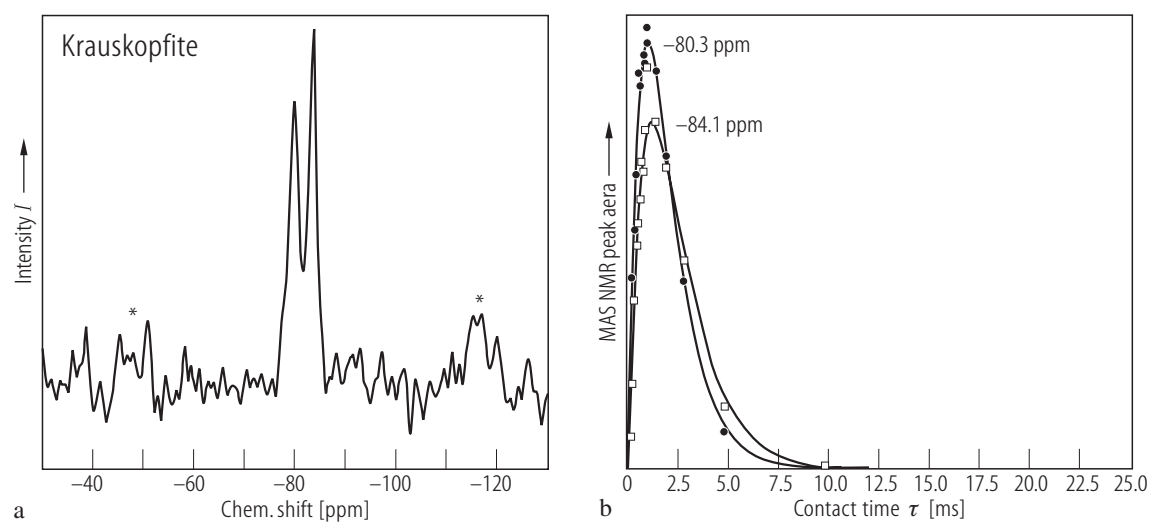


Fig. 10. Krauskopfite. (a) The ¹H - ²⁹Si cross-polarization MAS NMR spectra at $\tau = 2$ ms contact times. The Si-OH sites are emphasized. The spinning rate is 2.5 kHz with spinning sidebands indicated by (*). (b) Cross-polarization MAS integrated peak area vs. contact time τ . The curve for each site is labeled by its peak position [0001].